Organic & Biomolecular Chemistry

www.rsc.org/obc

Volume 10 | Number 21 | 7 June 2012 | Pages 4137–4300

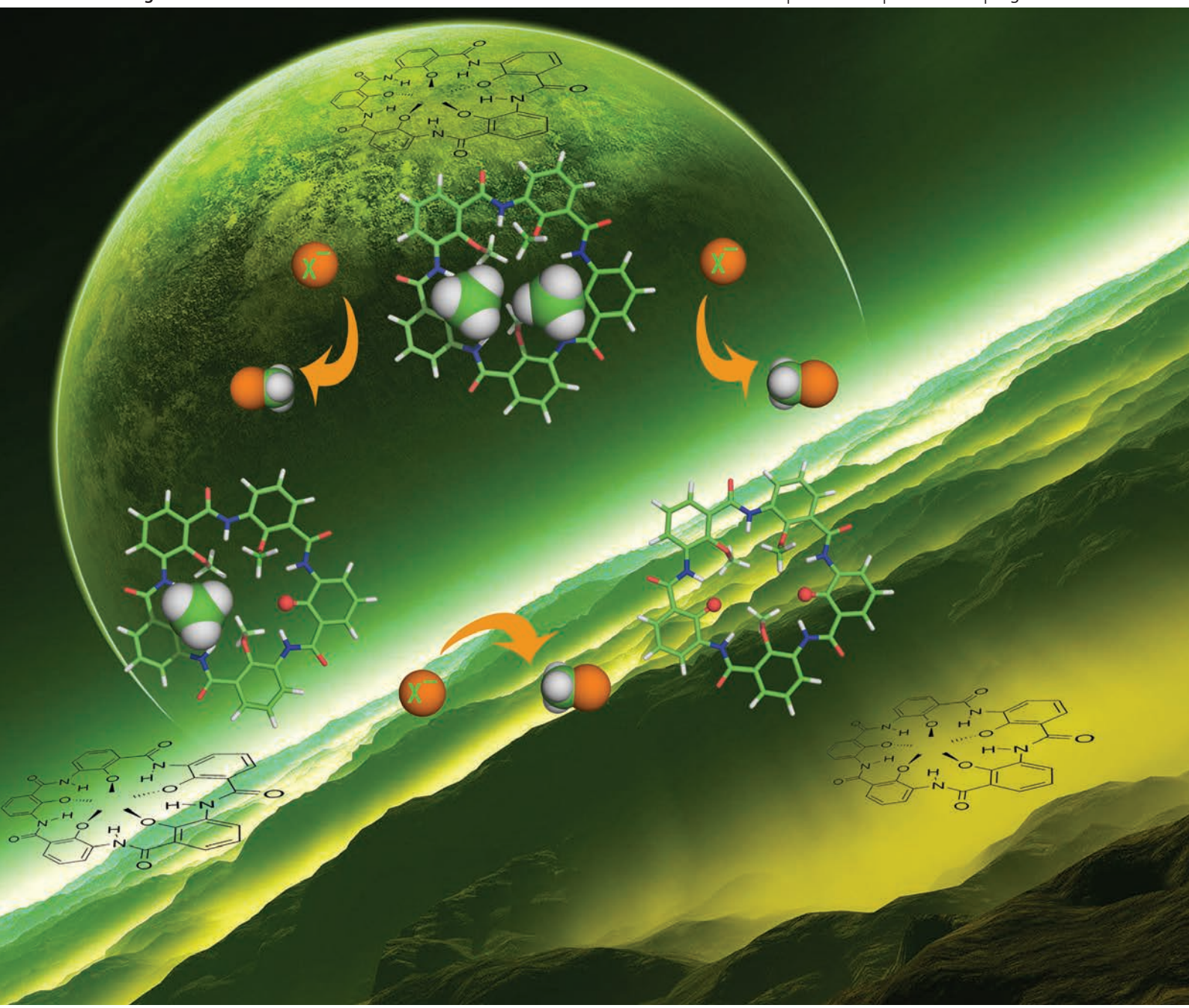

ISSN 1477-0520

RSC Publishing

PAPER

Huaqiang Zeng *et al.*

Folding-promoted TBAX-mediated selective demethylation of methoxybenzene-based macrocyclic aromatic pentamers

Organic & Biomolecular Chemistry

Dynamic Article Links

Cite this: *Org. Biomol. Chem.*, 2012, **10**, 4164

www.rsc.org/obc

PAPER

Folding-promoted TBAX-mediated selective demethylation of methoxybenzene-based macrocyclic aromatic pentamers

Zhiyun Du,[a] Bo Qin,[b] Chang Sun,[c] Ying Liu,[c] Xi Zheng,[a] Kun Zhang,[a] Allan H. Conney[a] and Huaqiang Zeng*[c]

Received 20th January 2012, Accepted 5th March 2012
DOI: 10.1039/c2ob25160d

Described in this study is the ability of tetrabutylammonium salts (TBAX) to mediate an efficient mono- or di-demethylation removing one or two out of five aromatic methoxy methyl groups situated in similar chemical microenvironments in a H-bonded macrocyclic aromatic pentamer. These demethylations are found to be both chemo- and regioselective, and promoted by the H-bonding directed folding of the macrocyclic backbone.

Introduction

A few outcomes on reactivity may be obtained *via* conformational pre-organization of organic backbones. Synthetic molecular containers,[1] on the one hand, enclose a 3D-shaped inner cavity, creating a confined nanoscale environment capable of altering the energy barrier for diverse chemical transformations. Prominent examples include the use of Rebek's cavitand molecules,[2] cyclodextrin,[1a,f,3a] calixarenes,[3b] and cucurbit[8]uril[3c–e] to promote or slow down[1i,3e] intended chemical reactions. In these cases, the reactivity of the trapped molecule rather than the host is altered. Foldamers, on the other hand, can fold into conformationally well-defined backbones caused primarily by non-covalent forces. Despite the highly repetitive nature of their folding backbones that are made up of repeating units of the same or similar types, a difference in the reactivity along the folding backbone containing a regular array of reactive sites is expected for repeating units of the same or similar types. The hitherto discovered examples include reactive sieving on methylation by Moore,[4a,b] selective N-oxidation[4c] and bromination[4d] of the pyridine-based helical oligoamides by Huc and selective hydrogenation of the carbonyl group of the 1,10-anthraquinone oligoamides by Chen *et al.*[4e] The perspective on such differential reactivities associated with foldamers is very inspiring, however, has been scarcely studied, particularly with respect to the extensive investigations already carried out on the container molecules.[1–3]

By utilizing inward-pointing H-bonding networks to rigidify the aromatic backbones, we have recently reported a series of crescent-shaped internally H-bonded foldamer molecules.[5,6] With a further backbone confinement *via* a covalent macrocyclization, the appropriately sized pentamers such as **1** can become circularly folded to arrive at a unique pentagon shape[5c–i,6a–c] that differs from diverse macrocycles reported by others.[7] The crystal structure of pentamer **1**[5c] reveals the presence of two sterically bulky caps made up of three and two methyl groups, respectively, covering either side of the pentamer plane (Fig. 1b). The

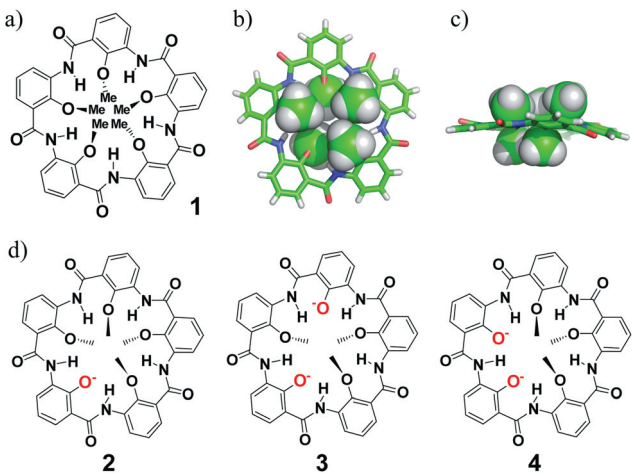

Fig. 1 (a) Structure of pentamer **1** with (b) top and (c) side views of its crystal structure, illustrating the steric crowding involving the interior methyl groups.[5c] (d) Structures of anionic pentamers **2**–**4**. The interior methyl groups in **2** point up and down alternately as revealed by the crystal structure.[5d] Both **3** and **4** as shown are the computationally most stable conformers, differing from others by the orientation of the interior methyl groups.

[a]*Allan H. Conney Laboratory for Anticancer Research, Guang Dong University of Technology, Guang Dong, 510006, China*
[b]*College of Chemistry and Chemical Engineering, Chongqing University, Chongqing, China 400030*
[c]*Department of Chemistry, National University of Singapore, 3 Science Drive 3, Singapore. E-mail: chmzh@nus.edu.sg; Fax: +65-6779-1691; Tel: +65-6516-2683*

unsymmetrical occurrence of the two steric caps twists the pentameric backbone and in the mean time, destabilizes the molecules due to the crowding involving the methyl groups by a computationally derived energetic penalty of 2–3 kcal mol^{-1} (see Results and discussion). A need to eliminate this energetic penalty may lead to differential reactivities of these interior methoxy groups toward demethylating agents, producing anionic pentamers **2–4** for the selective recognition of metal cations.[5d] Apart from releasing the steric crowdedness, eliminating methoxy methyl groups also generates intermediate anionic phenolates that lead to the formation of stronger intramolecular H-bonds[5d] with respect to those mediated by methoxy O-atoms. This should stabilize the resultant anionic pentamers. Additionally, the strong repulsive interactions among the newly generated negatively charged O-atoms may further prevent the excessive demethylation from happening, resulting in the selective removal of methoxy methyl groups at the energetically favored sites. In fact, the energetic destabilization of the pentamer by the two negatively charged *ortho* O-atoms can respectively amount to as large as 13.14, 6.55 and 5.62 kcal mol^{-1} in the gas phase, $CHCl_3$ and THF (**3** *vs.* **4** in Fig. 1, also see Results and discussion).

In our recent quest to examine the above hypothesis, we indeed showed that up to two out of five methyl groups situated in similar macrocyclic chemical microenvironments as in **1** can be selectively removed in chemo- and regioselective fashions promoted by TBACl-mediated folding-induced selective demethylations. More specifically, anionic pentamers **2** and **3** can be obtained in pure forms in 98% and 97% yields with the use of 20 and 5 equivalents of TBACl as the sole demethylating agent in HPLC grade chloroform (≤0.02% water) and tetrahydrofuran (<0.02% water), respectively.[5h]

In the present study, we have systematically looked into the solvent effects on the TBACl-mediated demethylations, and further looked into the demethylation efficiencies promoted by other TBAX salts, particularly TBABr in varying solvents. We show here that dianionic pentamer **3** can be produced in essentially pure form in yields of >95% in the majority of solvents studied using either TBACl or TBABr. Production of **3** proceeds *via* **2** as the intermediate by a two-step mechanism with the first chemoselective mono-demethylation being faster than the second regioselective mono-demethylation (Fig. 2a). The chemoselectivity primarily results from the folding-induced clustering of methoxyl methyl groups whose hydrophobic interactions computationally estimated to destabilize the pentamer by 2–3 kcal mol^{-1}. The regioselectivity predominantly arises from a necessity to reduce the strong repulsions among the negatively charged essentially non-mobile phenolate O-atoms as in **3** and **4**. This affords di-demethylated **3** that is more stable than **4** by 5.62 kcal mol^{-1} in THF. These computational molecular modeling results allow us to surmise that the first mono-demethylation occurs at one of the two methoxy sites *ortho* to each other on the more crowded side containing three methoxy groups, and the second mono-demethylation happens from the less crowded side at the methoxy group that is *meta* to the first demethylation site, producing the most stable regioisomer **3** and avoiding the generation of strongly repulsive negatively charged *ortho* oxygens as found in **4**.

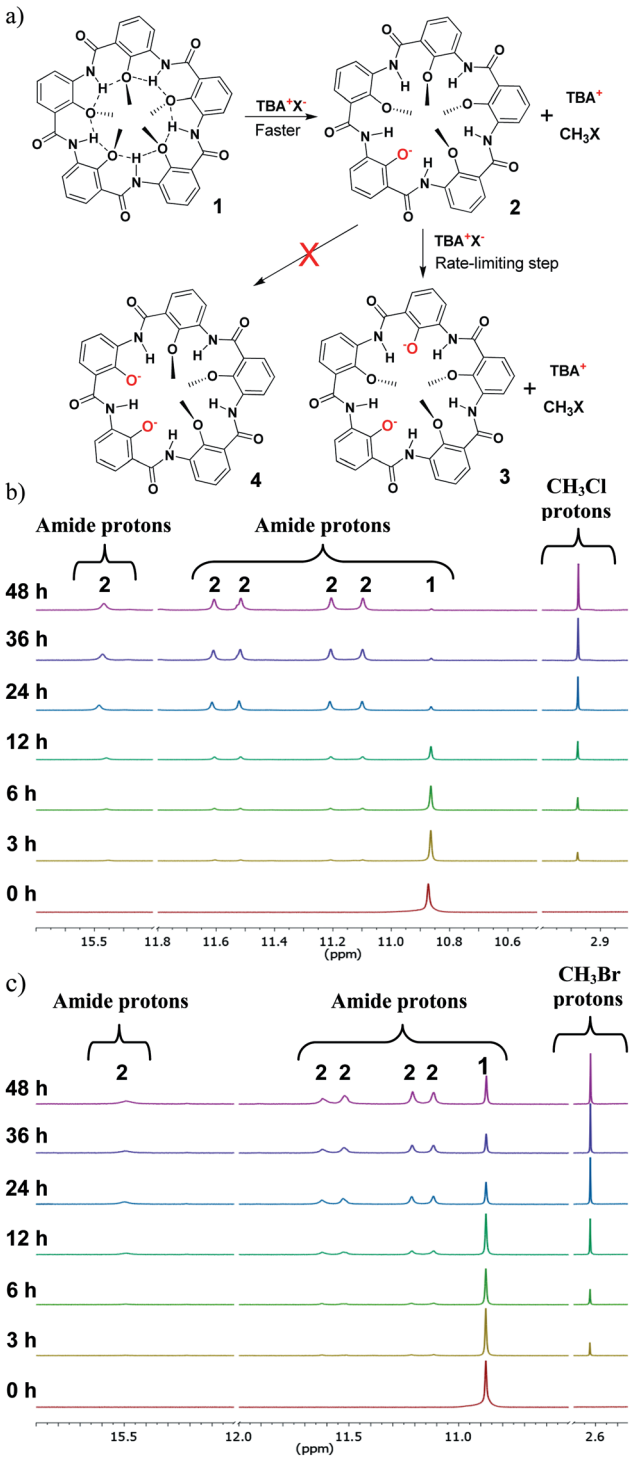

Fig. 2 (a) TBAX-mediated demethylating mechanism with the first chemoselective mono-demethylation faster than the second regioselective mono-demethylation, which can be validated by (b) and (c) ^{1}H NMR analyses of mono-demethylation products, *e.g.*, **2** and CH_3Cl[5h] or CH_3Br produced by treating **1** with 20 equivalents of TBACl or TBABr in $CDCl_3$. The peaks at 3.05 and 2.63 ppm belong to the methyl protons from CH_3Cl and CH_3Br, thereby confirming the demethylating mechanism illustrated in (a).

Table 1 Screening demethylating conditions[a] for the selective demethylation of methoxy groups present in circular pentamer **1**

Entry	Demethylating reagents	Solvent	Yield[b] (%)
1	CF_3COOH	NMP	—[c]
2	CF_3COOH/NaI	DMF	—[c]
3	TsOH	NMP	—[c]
4	TsOH/NaI	NMP	—[c]
5	$MeSO_3H$	THF	—[c]
6	Me_3SiH	THF or $CHCl_3$	—[c]
7	$AlCl_3$	CH_3CN	—[c]
8	$AlCl_3$, NaI	THF	—[c]
9	$AlCl_3$, TBACl	THF	—[c]
10	$AlCl_3$, TBABr	THF	—[c]
11	LiCl	THF	—[c]
12	1 M HCl	$CHCl_3$	—[c]
13	1 M HCl	THF	—[c]
14	1 M HCl	ether	—[c]
15	3 M HCl	AcOH	Trace of **2**[d]
16	3 M HCl	NMP	**1** : **2** : **3** = 52% : 37% : 11%
17	BBr_3	THF	—[c]
18	BBr_3	CH_2Cl_2	**1** : **2** : **3** = 94% : 4% : 2%
19	1 M BBr_3	CH_2Cl_2	Mixture[d,e]
20	HBr	NMP	Mixture[d,e]
21	HBr	AcOH	Trace of **2**[d]

[a] Reaction conditions: **1** (0.005 mmol), demethylating reagents (0.025 mmol or the specified concentration), solvent (1.0 mL), 60 °C, 12 h. [b] Yields determined by ^{1}H NMR. [c] No product can be detected. [d] Detected by MS. [e] Mixture containing up to four phenolate moieties that correspond to the removal of four methyl groups. NMP = *N*-methylpyrrolidone; TsOH = toluenesulfonic acid. In entry 12, the reaction was carried out at room temperature.

Results and discussion

TBAX-mediated demethylation and mechanism

Before our serendipitous discovery of TBACl as the sole demethylating reagent for selectively removing up to two methyl groups in **1**,[5h] various demethylating conditions were tested first to examine their ability to remove the interior methoxy methyl groups in **1** (Table 1). These demethylating conditions, in most cases (entries 1–14 and 17), fail to produce detectable amounts of hydroxyl-containing or anionic pentamers such as **2**–**4** (Fig. 2b), and in other cases (entries 16 and 18–20) result in a mixture of anionic pentamers containing up to four phenolate moieties with **1** remaining very significant. As an illustrative example from entry 16, the use of 3 M HCl in a polar solvent NMP produces **2** and **3** in 37% and 11% yield, respectively, with slightly more than half of the starting material remaining unreacted. The structural details of **2** and **3** were verified by comparing with the anionic pentamers previously made by deprotonating the interior hydroxyl groups using organic base TBAOH.[5d] The structure of **2** is further confirmed by determining its crystal structure that reveals a structure identical to that recently reported by us.[5d]

It was found later that the use of TBACl as the only demethylating reagent results in chemo- and regioselective demethylations, producing **2** or **3** in almost quantitative yields.[5h] The demethylation mechanism proceeds as shown in Fig. 2a whereby halide Cl^- anion attacks the methoxy carbon atom and removes the methyl group to produce a phenolate anion as found in **2** or **3**.[5h] This mechanism can be verified by ^{1}H NMR analysis of mono-demethylation products (Fig. 2b–c), demonstrating the formation of **2** and CH_3Cl[5h] or CH_3Br produced treating **1** with 20 equivalents of TBACl or TBABr in $CDCl_3$. It can be seen that mono-demethylation takes place faster in the presence of TBACl than TBABr. This may be due to the fact that the newly produced CH_3Br is a better methylating reagent than CH_3Cl, thereby converting the generated phenolate anion back into methoxy benzene faster than CH_3Cl.

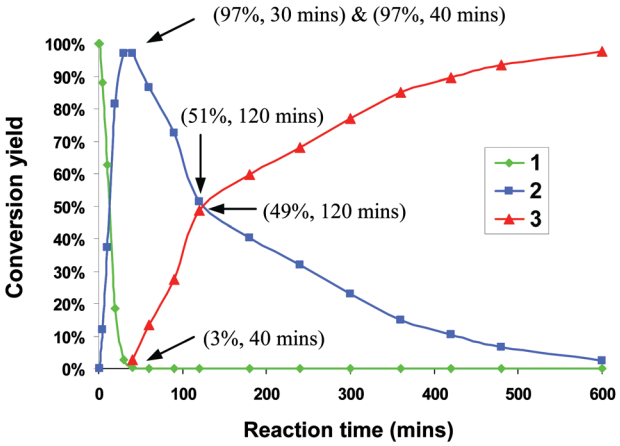

Fig. 3 ^{1}H NMR-based analysis of the reaction progress *vs.* reaction time by treating **1** with four equivalents of TABCl in THF at 60 °C, illustrating the conversion of **1** (green) to **3** (yellow) *via* **2** (blue) as the intermediate.

It is also very interesting to note that the demethylation proceeds faster in THF than in CH_3Cl, and both **2** and **3** can be produced in essentially pure forms that depend on the reaction time. As schematically illustrated in Fig. 3, a more detailed ^{1}H NMR-based analysis on the reaction product **3** produced by using 4 equivalents of TABCl in anhydrous THF shows that the di-demethylation reaction producing **3** proceeds in two steps with the first mono-demethylation faster than the second mono-demethylation (Fig. 2a). It is evidenced that transformation of ~97% of **1** into **2** is achieved in about 30 minutes, while converting **2** into **3** with an accumulated yield of 97% takes more than 500 minutes.

Expanding the scope of demethylation reactions

Encouraged by the solvent effect on TBACl-mediated demethylation that produces anionic **2** and **3** in essentially pure forms in $CHCl_3$ and THF, respectively, we were intrigued to investigate the products possibly generated by TBACl in other solvents as well as by other TBA halide salts in varying solvents.

Screening against TBA salts was first carried out in HPLC grade $CHCl_3$. In $CHCl_3$, only anionic **2** can be produced in yields of 99% (TBACl), 84% (TBABr), 52% (TBAI) and 0% (TBAF) as shown by us previously.[5h] A further screening was carried out in HPLC grade THF, a solvent where the demethylation reaction seems to be much faster. From Table 2, the demethylation efficiencies of these salts in terms of producing **3** can be ranked in the order of TBACl ≈ TBABr ≫ TBAF ≈

Table 2 Demethylating efficiencies of TBAX-mediated demethylation on the formation of anionic **3** from pentamer **1**[a]

			Yield[b] (%)		
Entry	TBAX	Solvent	**1**	**2**	**3**
1	TBAF	THF	66	0	34
2	TBACl	THF	0	2	98
3	TBABr	THF	1	2	97
4	TBAI	THF	67	0	33

[a] Reaction conditions: **1** (0.005 mmol), TBAX (5 equiv, 0.025 mmol), HPLC grade THF (1.0 mL), 60 °C, 12 h. [b] Yields determined by ^{1}H NMR.

Table 3 Solvent effects of TBACl/Br-mediated demethylation on the formation of anionic **2** and **3** from pentamer **1**[a,b]

			Yield[c,d] (%)		
Entry	TBAX	Solvent	**1**	**2**	**3**
1a	TBACl	CH_3CN	100	0	0
1b	TBABr		100	0	0
2a	TBACl	$CHCl_3$	90 (1)	10 (99)	0
2b	TBABr		77 (16)	23 (84)	0
3a	TBACl	DMSO	70 (0)	30 (11)	0 (89)
3b	TBABr		47 (1)	53 (7)	0 (92)
4a	TBACl	DMF	1 (1)	95 (2)	4 (97)
4b	TBABr		7 (0)	89 (5)	4 (95)
5a	TBACl	THF	0	2	98
5b	TBABr		1	2	97
6a	TBACl	Ethyl acetate	1	6	93
6b	TBABr		0 (3)	30 (10)	70 (87)
7a	TBACl	Acetone	61 (1)	39 (2)	0 (97)
7b	TBABr		1 (2)	72 (2)	27 (96)
8a	TBACl	Toluene	84 (0)	12 (0)	4 (99)
8b	TBABr		1	1	98
9a	TBACl	Dioxane	1 (0)	66 (0)	33 (99)
9b	TBABr		1 (0)	33 (4)	66 (96)
10a	TBACl	NMP[e]	0	85	15
10b	TBABr		0	46	54

[a] Reaction conditions: **1** (0.005 mmol), TBACl/Br (5 equiv, 0.025 mmol), AR or HPLC grade solvent (1.0 mL), 60 °C, 12 h. [b] Dichloromethane was not tested due to its low boiling point of 39.6 °C. [c] Yields determined by ^{1}H NMR. [d] The yields in brackets were obtained by using 20 equivalents of TBACl/Br salts at 60 °C after 48 h. [e] The use of 20 equivalents of TBACl/Br in this solvent led to a mixture of anionic pentamers with **3** as the major product.

TBAI. Accordingly, TBACl and TBABr were chosen for the subsequent screening of solvent effects on the demethylation reactions by employing 5 equivalents of TBACl or TBABr at 60 °C for 12 hours. Among the ten solvents tested, no demethylation occurs in acetonitrile (entry 1, Table 3). Although the mono-demethylation takes place to low extents in $CDCl_3$ with the use of 5 equivalents of TBACl or TBABr, the reaction proceeds to much greater extents after two days by using 20 equivalents of either TBACl or TBABr (entry 2). Similar to TBACl, monitoring the reaction products by ^{1}H NMR shows that TBABr-mediated demethylation in $CDCl_3$ exclusively affords **2** with a 84% yield (entry 2b) by a mechanism shown in Fig. 3a. Producing **2** as the major product is also seen when DMSO was used as the reaction medium: **2** was selectively produced in 30% and 53% in the presence of 5 equivalents of TBACl and TBABr, respectively. In DMF, the predominant product generated by using TBACl and TBABr is also **2** with a very insignificant production of **3** (entry 4, Table 3).

The above selective production of **2** by demethylation in $CHCl_3$, DMSO and DMF was completely suppressed in other solvents including THF (entry 5), ethyl acetate (entry 6) and toluene (entry 8b). Under these conditions, the demethylation reaction is also highly regioselective, giving rise to **3** rather than **4** *via* **2** as the intermediate pentamer. In all the other entries 7–10 where a mixture of **2** and **3** co-exist in the reaction, **3** is similarly produced *via* **2**. This can be evidenced by almost quantitative conversions of **1** into **3** upon increasing the use of TBACl or TBABr from 5 to 20 equivalents (see yields in brackets of entries 7–10). A closer look into the solvent effects reveal that the product distribution pattern produced by TBACl is of the same general trend as that by TBABr in CH_3CN, $CHCl_3$, DMSO, DMF THF and ethyl acetate (entries 1–6). Specifically, predominant production of either **2** or **3** can be equally achieved by using either TBACl or TBABr. In other solvents including acetone, toluene, dioxane and NMP (entries 7–10), reciprocal trends in product distribution are observed in the presence of five equivalents of TBACl/Br. For example, while **2** is the only product produced by TBACl in acetone (entry 7a), both **2** and **3** can be obtained by TBABr in acetone (entry 7b). For another example, **2** as a major product obtained by TBACl becomes the minor product when TBABr is used (entries 9 and 10). In short, except for CH_3CN whereby no demethylation occurs and $CHCl_3$ whereby mono-demethylation happens exclusively to produce **2**, pure **3** can be obtained in all the other solvents with the use of 20 equivalents of TBACl/Br.

Computational insights into chemo- and regioselectivity

Initially, we thought that screening the various conditions summarized in Table 3 might make it possible to produce anionic **4** or other anionic pentamers containing more than two phenolate anions in essentially pure forms for fine-tuning the cation-binding abilities of anionic pentamers as recently demonstrated by us.[5d] It turns out that these TBAX-mediated demethylations are very selective, eliminating only one or two methoxy methyl groups at specific positions to produce anionic **2** or **3**, respectively.

As illustrated in Fig. 4a, a total of five anionic conformers can be generated by removing one methyl group from pentamer **1**. These five conformers can be classified into three conformer types **2**, $\mathbf{2_{II}}$ and $\mathbf{2_{III}}$. Conformers **2** and $\mathbf{2_{II}}$ both are composed of two conformers that are equal in energy and experimentally cannot be differentiated from each other. Chemoselectivity refers to the selective production of conformer **2**, rather than $\mathbf{2_{II}}$ and $\mathbf{2_{III}}$. This has been proven experimentally. Although the difference in stability among anionic **2**, $\mathbf{2_{II}}$ and $\mathbf{2_{III}}$ is $\leq$1.31 kcal mol^{-1}, the energy barriers in THF for transforming **2** into $\mathbf{2_{II}}$ (or its other energetically equivalent forms) or $\mathbf{2_{II}}$ into $\mathbf{2_{III}}$ (or its other energetically equivalent forms) were determined to be as large as 9.34 and 13.00 kcal mol^{-1} (Fig. 4a), respectively, at the B3LYP/6-311+G(d,p) level. These high energy barriers stem from (1) strong repulsions among methyl groups and (2)

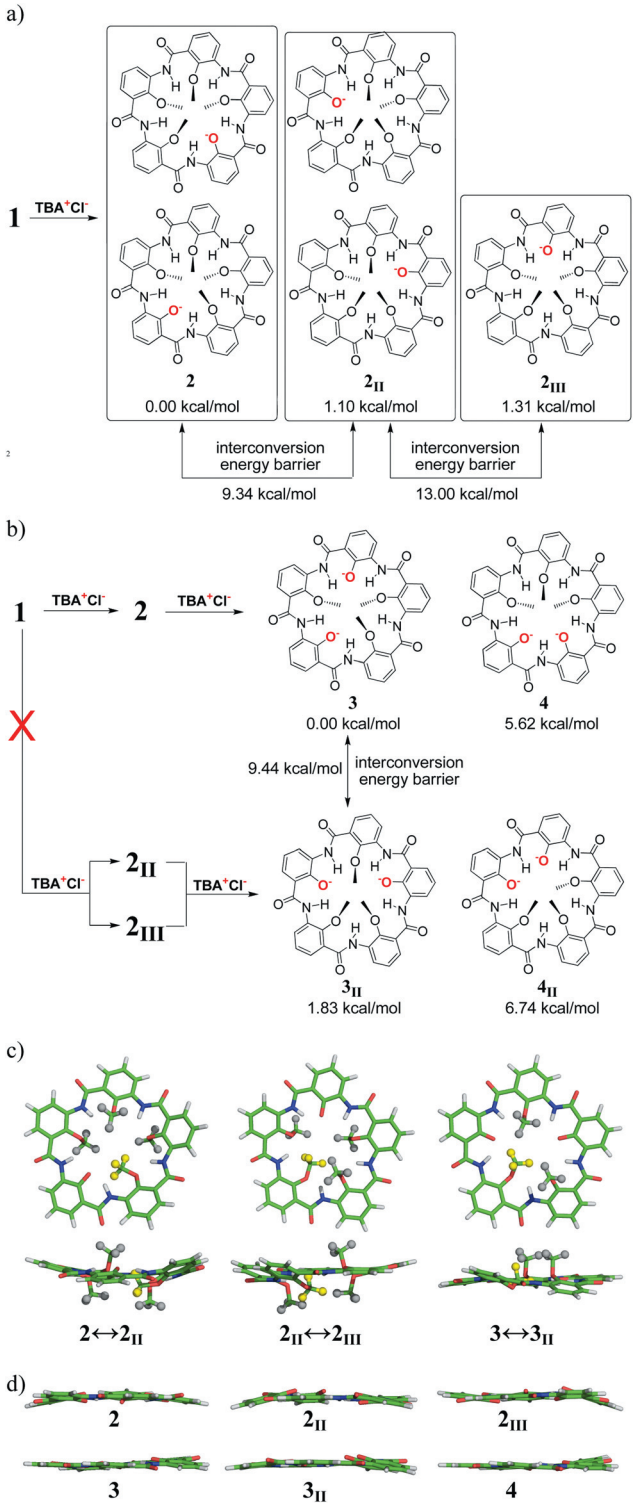

Fig. 4 (a) Mono-demethylation of **1** is chemoselective, producing **2** rather than $\mathbf{2_{II}}$ and $\mathbf{2_{III}}$. (b) Di-demethylation occurs sequentially *via* **2**, not $\mathbf{2_{II}}$–$\mathbf{2_{III}}$, to regioselectively produce **3**, but not **4**. The energies in kcal mol^{-1} in (a) and (b) are obtained using THF as the explicit solvent and normalized against conformers **2** and **3**, respectively. (c) Top and side views of computationally determined transition states, dictating the inter-conversions between **2** and $\mathbf{2_{II}}$, between $\mathbf{2_{II}}$ and $\mathbf{2_{III}}$, and between **3** and $\mathbf{3_{II}}$ by flipping the methoxy groups in yellow. (d) Side views of the optimized planar backbones for **2**, $\mathbf{2_{II}}$, $\mathbf{2_{III}}$, **3**, $\mathbf{3_{II}}$ and **4**. Other energetically equivalent mirror-images or isomers are not considered.

Table 4 Computationally derived relative energies among conformers $\mathbf{1_I}$–$\mathbf{1_{IV}}$ in gas phase and in the explicit solvents using density functional theory at the B3LYP/6-31G* level with their single point energies calculated at the level of B3LYP/6-311+G**

	Relative energies (kcal mol^{-1})			Energetic parameters[a] (kcal mol^{-1})		
Solvent (dielectric constant)	$E_{II} - E_I$	$E_{III} - E_I$	$E_{IV} - E_I$	E_M	E_O	ΔE^b
Gas phase	2.94	3.47	8.03	0.36	1.83	2.91
THF (7.58)	2.68	3.03	6.99	0.27	1.61	2.42
$CHCl_3$(4.9)	2.59	3.02	6.83	0.27	1.57	2.40
Acetone (20.7)	2.78	3.11	6.66	0.18	1.57	2.12
CH_3CN (36.64)	2.80	2.97	6.47	0.14	1.54	1.98
DMSO (46.7)	2.78	3.04	6.34	0.13	1.52	1.91

[a] Obtained by using Mathematica program.[9] [b] Destabilizing energy caused by interior methoxy methyl groups.

pentameric backbones that are more twisted in the transition states (Fig. 4c) than the nearly planar backbones found in **2**, $\mathbf{2_{II}}$ and $\mathbf{2_{III}}$ (Fig. 4d), and suggest that once anionic **2** is produced, it may stay as the major conformer in solution with $\mathbf{2_{II}}$ and $\mathbf{2_{III}}$ remaining less than 1%.

Similarly, four types of anionic conformers, *i.e.*, **3**, $\mathbf{3_{II}}$, **4**, and $\mathbf{4_{II}}$ can be generated by removing two methyl groups from pentamer **1** (Fig. 4b). Please note that **3** and $\mathbf{4_{II}}$ each contain a set of four energetically equivalent conformers, and $\mathbf{3_{II}}$ and **4** each contain a set of two energetically equivalent conformers. Since chemoselectivity of the reaction allows for the production of conformer **2**, the presence of conformers $\mathbf{3_{II}}$ and $\mathbf{4_{II}}$ *via* either $\mathbf{2_{II}}$ or $\mathbf{2_{III}}$ as the intermediate pentamer in the reaction is unlikely; $\mathbf{3_{II}}$ and $\mathbf{4_{II}}$ therefore will not be subjected to further discussion. Regioselectivity then refers to the selective production of conformer **3**, rather than **4**. This has also been proven experimentally. In addition to a large difference of 5.62 kcal mol^{-1} in energy in THF between **3** and **4**, the energetic barrier of as high as 9.44 kcal mol^{-1} (Fig. 4b–d) for transforming **3** into $\mathbf{3_{II}}$ further suggests **3** as the predominant conformer in solution.

From Fig. 2c, it takes on estimate ~13 and ~120 minutes, respectively, to convert the first 50% of **1** into **2** and of **2** into **3**. Then why is the first mono-methylation reaction producing **2** rapidly and faster than the second mono-demethylation reaction that constitutes the rate-limiting step in producing **3** (Fig. 3)? This difference in reaction rate can be understood on the basis of (1) ring strain arising from the interior methyl groups, (2) the repulsive interactions between methoxy O-atoms and negatively charged phenolate O-atoms, and (3) strong electrostatic repulsion between negatively charged phenolate O-atoms.

As discussed below in the section of "Origin of chemoselectivity", repulsive *ortho* $CH_3\cdots CH_3$ and *meta* $CH_3\cdots CH_3$ interactions each destabilize pentamer **1** by 1.52–1.61 and 0.13–0.27 kcal mol^{-1} (Table 4), respectively. That is to say, transforming **1** to **2** by the first mono-demethylation reaction therefore results in a release of ring strain worth 1.65–2.19 kcal mol^{-1} upon eliminating one E_O and one E_M interaction (Fig. 4a and 5a). This process is unfavorably accompanied by the two repulsive interactions among the newly generated negatively charged phenolate O-atoms and its two neighboring methoxy

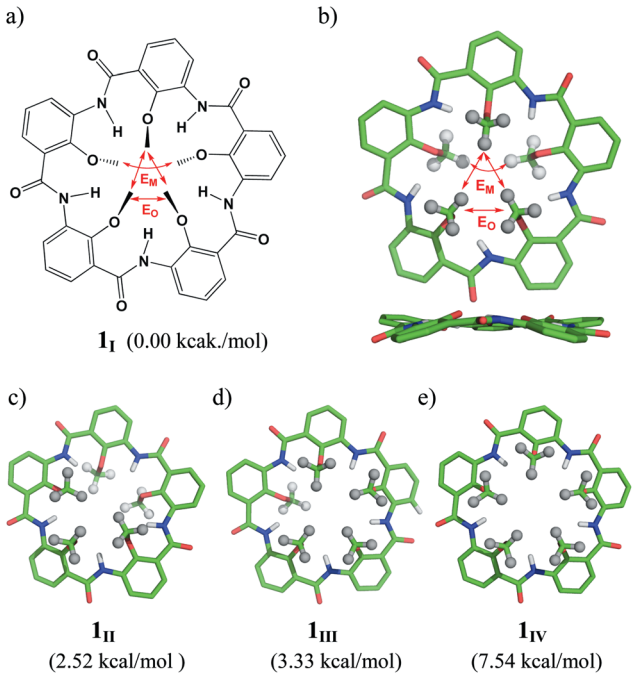

Fig. 5 Computationally optimized four conformers derived from pentamer **1** that are dependant on the orientation of the interior methoxy methyl groups in the gas phase. (a) Structure of conformer $\mathbf{1_I}$; E_O = repulsive interaction between the two methyl groups in *ortho* positions; E_M = repulsive interaction between two *meta*-methyl groups; one E_O and three E_M interactions can be found in $\mathbf{1_I}$. (b) Top and side views of the computationally optimized structure of conformer $\mathbf{1_I}$. (c–d) *Ab initio*-optimized structures of conformers $\mathbf{1_{II}}$–$\mathbf{1_{IV}}$ with their relative energies normalized against the most stable conformer $\mathbf{1_I}$. Their relative energies in kcal mol^{-1} in the gas phase are normalized against the most stable conformer $\mathbf{1_I}$. Swapping the interior methyl groups yields mirror-images of another four conformers $\mathbf{1_I}$–$\mathbf{1_{IV}}$ that are equal in energy and not considered here.

O-atoms (distances among the *ortho* O-atoms ≈3.4 Å). Comparatively, producing **3** from **2** (Fig. 4b) in the second mono-demethylation step allows the release of a much smaller ring strain worth about 0.13–0.36 kcal mol^{-1} by removing one E_M interaction; this process undesirably introduces four repulsive interactions among two phenolate O-atoms and two adjacent methoxy O-atoms as well as one additional repulsive interaction between two phenolate O-atoms (distance = 5.6 Å). The immediate implication from this increased energetic penalty associated with the second mono-demethylation process is a slower reaction rate as compared to that of the first mono-demethylation process.

Origin of chemoselectivity

In this section, we will use *ab initio* quantum mechanics to help provide some energetic insights into the origin of the chemoselectivity that leads to the selective production of anionic **2** rather than its other closely related conformers $\mathbf{2_{II}}$ and $\mathbf{2_{III}}$. The computational work was carried out at the level of B3LYP/6-31G* with the single point energy calculation carried out at the B3LYP/6-311+G(d,p) level.[8]

As elaborated below, it is the repulsive interactions among the interiorly arrayed hydrophobic methyl groups (Fig. 1b–c) that are responsible for the observed chemoselectivity, leading to the preferred formation of energetically more stable anionic **2**.

The H-bond enforced circular pentamer **1** contains two interiorly aligned hydrophobic caps made up of two and three methyl groups, respectively, covering either side of the pentamer plane (Fig. 1b, 1c and 5).[5c] The hydrophobic nature and bulkiness of the methyl groups on the same side make these methyl groups repel each other, leading to a slightly twisted non-planar backbone and destabilizing the molecule to a certain degree. These repulsive $CH_3\cdots CH_3$ interactions engaging methyl groups can be classified to have two types according to whether the interacting methyl groups are *ortho* (E_O, Fig. 5a) or *meta* (E_M, Fig. 5a) to each other, with the former being stronger than the latter. To quantify the values of these repulsions, the computationally derived relative energies were used with the assumptions being that (i) the same type of repulsive interaction destabilizes the pentamer to an equal extent and (ii) the cross-plane interactions among methyl protons can be neglected. In Fig. 5, a total of four different conformations for circular pentamer **1**, depending on the orientation of interior methoxy groups, were fully optimized using density functional theory at the B3LYP/6-31G* level in gas phase. Circular conformer $\mathbf{1_I}$, bearing five methoxy groups spatially arranged in an up–down–up–down–up fashion, is found to be the most stable and the only conformation that is also found in the solid state.[5c] The other three conformers $\mathbf{1_{II}}$–$\mathbf{1_{IV}}$, possessing alternative side chain orientations, are destabilized by 2.9–8.0 kcal mol^{-1} with respect to $\mathbf{1_I}$ (Fig. 5c–e and Table 4). The same calculation was then extended to some selected solvent systems to examine the solvent effect on the energetic profiles of $CH_3\cdots CH_3$ interactions (Table 4).

By defining E = energy of **1** in the absence of repulsive interactions among interior methyl groups, E_O = destabilizing energy resulting from *ortho*-methyl groups, E_M = destabilizing energy resulting from *meta*-methyl groups, u = methyl group in up position, and d = methyl group in down position, the energies of the four conformers in Fig. 5 can be expressed as follows:

E = Energy of **1** in the absence of $CH_3\cdots CH_3$ interactions
$E_I = E - E_O - 3E_M$ for $\mathbf{1_I}$ with a uduud arrangement
$E_{II} = E - 3E_O - E_M$ for $\mathbf{1_{II}}$ with a uuudd arrangement
$E_{III} = E - 3E_O - 3E_M$ for $\mathbf{1_{III}}$ with a uuuud arrangement
$E_{IV} = E - 5E_O - 5E_M$ for $\mathbf{1_{IV}}$ with a uuuuu arrangement

The above equations can be rearranged as eqn (1)–(4), where all the E values are taken as positive values, and ΔE is the destabilizing energy caused by interacting methyl protons in conformer $\mathbf{1_I}$ that involves one E_O and three E_M:

$$E_O + 3E_M = E_I - E = \Delta E \quad (1)$$

$$3E_O + E_M = E_{II} - E = \Delta E + (E_{II} - E_I) \quad (2)$$

$$3E_O + 3E_M = E_{III} - E = \Delta E + (E_{III} - E_I) \quad (3)$$

$$5E_O + 5E_M = E_{IV} - E = \Delta E + (E_{IV} - E_I) \quad (4)$$

The relative energies among the four conformers **I–IV** in both the gas phase and explicit organic solvents of varying types were calculated and listed in Table 4. Substituting these relative energies into eqn (1)–(4), followed by fitting the resulting equations using Mathematica program,[9] yielded the respective values for

Table 5 Computationally derived relative energies, ΔE, among various conformers in THF at the B3LYP/6-31G* level with their single point energies calculated at the B3LYP/6-311+G** level *vs.* ΔE* that refers to the relative energies obtained by substituting the E_M and E_O values into the equations expressing a difference in E_M and E_O interactions as observed in the conformers

	$\mathbf{2 - 2_{II}}$	$\mathbf{2 - 2_{III}}$	$\mathbf{3 - 3_{II}}$	$\mathbf{4 - 4_{II}}$
ΔE (kcal mol^{-1})	−1.10	−1.31	−1.83	−1.12
ΔE* (kcal mol^{-1})	−1.61	−1.34	−1.88	−1.34
Relative error[a]	32%	2.2%	2.7%	16%

[a] Defined as $(\Delta E - \Delta E^*)/\Delta E^*$.

E_O, E_M and ΔE compiled in Table 4. Inspection of data from Table 4 reveals that the interacting energy between *meta*-methyl protons, E_M, is quite sensitive to solvent polarity and decreases upon increasing solvent polarity from benzene to DMSO, while solvents exert much less influence onto the interaction between *ortho*-methyl protons. The respective values of E_O and E_M in THF were determined to be 1.61 and 0.27 kcal mol^{-1}. That is to say, every repulsive *ortho* or *meta* $CH_3\cdots CH_3$ interaction destabilizes **1** by 1.61 or 0.27 kcal mol^{-1}, respectively. In other solvents, the E_O and E_M range from 1.52–1.83 kcal mol^{-1} and 0.13–0.36 kcal mol^{-1}, respectively. From these values, it can be estimated that the five interior methyl groups energetically destabilize **1** by about 2–3 kcal mol^{-1} regardless of solvents used. Therefore, if the mono-demethylation takes place at one of the two methoxy methyl groups that are *ortho* to each other from the more crowded site, resulting in the formation of anionic **2** where one *ortho* and one *meta* $CH_3\cdots CH_3$ interactions are eliminated, the folding-induced strain can be maximally released with regard to the removal of any one of the other three methoxy groups that eliminates only *meta* $CH_3\cdots CH_3$ interaction, producing either $\mathbf{2_{II}}$ or $\mathbf{2_{III}}$ (Fig. 4). From Fig. 4, it can be seen that **2**, $\mathbf{2_{II}}$ and $\mathbf{2_{III}}$ contain $2E_M$, $2E_M + 1E_O$, and $1E_M + 1E_O$, respectively. The absence of E_O repulsion in **2** makes **2** energetically more stable than $\mathbf{2_{II}}$ and $\mathbf{2_{III}}$ by 1.52–1.83 and 1.30–1.47 kcal mol^{-1}, respectively. This partially explains why TBAX is able to demethylate the methoxy methyl group(s) in **1** that are quite crowded, but not the methoxy methyl group in monomer **5**, a macrocyclic repeating unit of **1** as recently reported by us.[5h] A decreased nucleophilicity of the phenolate anions that participate in the formation of stronger intramolecular H-bonds[5d] constitutes another reason why TBAX can mediate the removal of methoxy methyl groups and the resultant phenolate anions do not easily undergo further alkylation with the *in situ* generated CH_3X molecules.

The dependability of the values for E_M and E_O derived on the basis of the various conformers of **1** by using the Mathematica program can be scrutinized by cross-checking with the relative energies among conformers **2**, $\mathbf{2_{II}}$ and $\mathbf{2_{II}}$, between conformers **3** and $\mathbf{3_{II}}$, and between conformers **4** and $\mathbf{4_{II}}$ that were solely determined by *ab initio* computation at the B3LYP/6-31G* level with their single point energies calculated at the B3LYP/6-311+G** level in THF. From the data compiled in Table 5, it becomes clear to us that the values for E_M and E_O listed in Table 4 can be used to reliably estimate the relative stabilities among various conformers (Table 5). Even though the presence of negatively charged O-atoms possibly may result in large discrepancies between ΔE and ΔE*, such a discrepancy is only observed between **2** and $\mathbf{2_{II}}$. In the other three cases studied, the relative errors between the computationally determined (ΔE) and estimated (ΔE*) values are much smaller, an evidence of good reliability of the values obtained for E_M and E_O. Correspondingly, this reliability strongly substantiates the calculated value of 2–3 kcal mol^{-1}, accounting for the destabilization of the aromatic **1** by its five interior methyl groups. Of further note is that anionic $\mathbf{2_{II}}$ is even more stable than $\mathbf{2_{III}}$ for a reason we don't know yet.

Origin of regioselectivity

Considering a difference of 13.14, 6.55, 5.62, 3.24 and 3.03 kcal mol^{-1} in energy between anionic **3** and **4** (Fig. 4b) in the gas phase, $CHCl_3$, THF, CH_3CN and DMSO, respectively, the regioselective transformation of **2** into **3** rather than **4** becomes very obvious: the process producing **3** is energetically more advantageous than that producing **4** by 3.03–13.14 kcal mol^{-1}. Therefore, after the first chemoselective demethylation reaction, the second region-selective demethylation preferentially takes place at the methoxy group *meta* to the first demethylation site, avoiding producing strongly repulsive *ortho* O-atoms. The existence of strongly repulsive interactions arising from the two negatively charged *ortho* O-atoms can be substantiated by a small difference of 1.25 kcal mol^{-1} in energy in THF between pentamers **3** and **4** in their doubly protonated forms where the two phenolate anions are protonated to re-generate two neutral hydroxyl groups, resulting in the elimination of repulsive interactions between negatively charged anionic O-atoms. Furthermore, despite the fact that anionic **3** is computationally more stable than anionic **4** by 5.62 kcal mol^{-1} in THF, the doubly protonated pentamer **4** turns out to be more stable than the doubly protonated pentamer **3** by 1.25 kcal mol^{-1} in THF.

Conclusions

We document here an efficient demethylation protocol based on the use of TBACl/Br to achieve the chemo- and regioselective removal of the interior methoxy methyl groups, transforming aromatic pentamer **1** into anionic **2** or **3** in almost quantitative yields in varying solvents. The TBAX-mediated demethylation takes place largely as a result of (1) steric hindrance among interior methyl groups that destabilizes the molecule by 2–3 kcal mol^{-1} and (2) a decreased nucleophilicity of the resultant phenolate anions that participate in the formation of stronger intramolecular H-bonds.[5d] By combining with the one-pot synthesis of pentamer **1** and other analogous pentamers in one step in ~50% yields,[5e,f] the currently established TBACl/Br-mediated demethylation protocol now allows for the generation of anionic **2** or **3** in just two steps with an overall yield approaching 50%. This "greener" production compares very favorably with the stepwise procedure previously reported by us that involves more than 16 steps in less than 1% yields after months of effort.[5d] The ease of synthetic access to anionic pentamers such as **3** (perhaps **4**[5d] in the near future) is important given their proven abilities to tightly bind alkali metal ions, and to differentiate between

Na^+/K^+ and Rb^+/Cs^+ ions in a highly selective fashion.[5d] This provides a strong drive for us to explore different methodologies in order to efficiently generate pentamers containing alternative arrays of hydroxyl groups in their cation-binding interiors to fine-tune their cation-binding affinities and selectivities. The availability of these diverse demethylation protocols should greatly facilitate the speedy evolution of cation-binding pentamers and eventually synthetic ion channels that can discriminate Na^+ against K^+ ions, both of which are biologically important.

Acknowledgements

Financial supports by National Research Foundation Competitive Research Programme Grant (R-154-000-529-281 to H.Z.), Environment and Water Industry Development Council and Economic Development Board (SPORE, COY-15-EWI-RCFSA/N197-1 to H.Z.) and National Natural Science Foundation of China (21042003 to Z.D. and 21172046 to K.Z.) is gratefully acknowledged.

Notes and references

1 (*a*) R. Breslow, *Acc. Chem. Res.*, 1980, **13**, 170; (*b*) N. Timmerman, K. G. A. E. A. Brinks, W. Verboom, F. C. J. M. van Veggel, W. P. van Hoorn and D. N. Reinhoudt, *Angew. Chem., Int. Ed. Engl.*, 1995, **34**, 132; (*c*) J. C. Ma and D. A. Dougherty, *Chem. Rev.*, 1997, **97**, 1303; (*d*) M. M. Conn and J. Rebek, Jr., *Chem. Rev.*, 1997, **97**, 1647; (*e*) K. A. Connors, *Chem. Rev.*, 1997, **97**, 1325; (*f*) R. Breslow and S. D. Dong, *Chem. Rev.*, 1998, **98**, 1997; (*g*) J. Rebek, Jr., *Acc. Chem. Res.*, 1999, **32**, 278; (*h*) R. Warmuth and J. Yoon, *Acc. Chem. Res.*, 2001, **34**, 95; (*i*) D. M. Vriezema, M. C. Aragones, J. A. A. W. Elemans, J. J. L. M. Cornelissen, A. E. Rowan and R. J. M. Nolte, *Chem. Rev.*, 2005, **105**, 1445; (*j*) Z. Laughrey and B. C. Gibb, *Chem. Soc. Rev.*, 2011, **40**, 363; (*k*) X.-H. Tian and C.-F. Chen, *Org. Lett.*, 2010, **12**, 524; (*l*) X.-H. Tian, X. Hao, T.-L. Liang and C.-F. Chen, *Chem. Commun.*, 2009, 6771; (*m*) M. Xue and C.-F. Chen, *Chem. Commun.*, 2008, 6128; (*n*) X.-H. Tian and C.-F. Chen, *Chem.–Eur. J.*, 2010, **16**, 8072; (*o*) M. Xue, Y.-S. Su and C.-F. Chen, *Chem.–Eur. J.*, 2010, **16**, 8537.

2 (*a*) J. Rebek, *Acc. Chem. Res.*, 2009, **42**, 1660; (*b*) F. R. Pinacho Crisostomo, A. Lledo, S. R. Shenoy, T. Iwasawa and J. Rebek, *J. Am. Chem. Soc.*, 2009, **131**, 7402.

3 (*a*) S. Hu, J. Li, J. Xiang, J. Pan, S. Luo and J.-P. Cheng, *J. Am. Chem. Soc.*, 2010, **132**, 7216; (*b*) C. D. Gutsche, *Acc. Chem. Res.*, 1983, **16**, 161; (*c*) C. Klock, R. N. Dsouza and W. M. Nau, *Org. Lett.*, 2009, **11**, 2595; (*d*) R. Kulasekharan, R. Choudhury, R. Prabhakar and V. Ramamurthy, *Chem. Commun.*, 2011, **47**, 2841; (*e*) L. S. Berbeci, W. Wang and A. E. Kaifer, *Org. Lett.*, 2008, **10**, 3721.

4 (*a*) R. A. Smaldone and J. S. Moore, *J. Am. Chem. Soc.*, 2007, **129**, 5444; (*b*) R. A. Smaldone and J. S. Moore, *Chem. Commun.*, 2008, 1011; (*c*) C. Dolain, C. L. Zhan, J. M. Leger, L. Daniels and I. Huc, *J. Am. Chem. Soc.*, 2005, **127**, 2400; (*d*) K. Srinivas, B. Kauffmann, C. Dolain, J. M. Leger, L. Ghosez and I. Huc, *J. Am. Chem. Soc.*, 2008, **130**, 13210; (*e*) H.-Y. Hu, J.-F. Xiang, J. Cao and C.-F. Chen, *Org. Lett.*, 2008, **10**, 5035.

5 For methoxybenzene-based foldamers, see: (*a*) Y. Yan, B. Qin, Y. Y. Shu, X. Y. Chen, Y. K. Yip, D. W. Zhang, H. B. Su and H. Q. Zeng, *Org. Lett.*, 2009, **11**, 1201; (*b*) Y. Yan, B. Qin, C. L. Ren, X. Y. Chen, Y. K. Yip, R. J. Ye, D. W. Zhang, H. B. Su and H. Q. Zeng, *J. Am. Chem. Soc.*, 2010, **132**, 5869; (*c*) B. Qin, X. Y. Chen, X. Fang, Y. Y. Shu, Y. K. Yip, Y. Yan, S. Y. Pan, W. Q. Ong, C. L. Ren, H. B. Su and H. Q. Zeng, *Org. Lett.*, 2008, **10**, 5127; (*d*) B. Qin, C. L. Ren, R. J. Ye, C. Sun, K. Chiad, X. Y. Chen, Z. Li, F. Xue, H. B. Su, G. A. Chass and H. Q. Zeng, *J. Am. Chem. Soc.*, 2010, **132**, 9564; (*e*) B. Qin, W. Q. Ong, R. J. Ye, Z. Y. Du, X. Y. Chen, Y. Yan, K. Zhang, H. B. Su and H. Q. Zeng, *Chem. Commun.*, 2011, **47**, 5419; (*f*) B. Qin, C. Sun, Y. Liu, J. Shen, R. J. Ye, J. Zhu, X.-F. Duan and H. Q. Zeng, *Org. Lett.*, 2011, **13**, 2270; (*g*) B. Qin, S. Shen, C. Sun, Z. Y. Du, K. Zhang and H. Q. Zeng, *Chem.–Asian J.*, 2011, **6**, 3298; (*h*) B. Qin, L. Jiang, S. Shen, C. Sun, W. Yuan, S. F. Y. Li and H. Q. Zeng, *Org. Lett.*, 2011, **13**, 6212; (*i*) Y. Liu, B. Qin and H. Q. Zeng, *Sci. China: Chem.*, 2012, **55**, 55.

6 For fluorobenzene-based foldamers, see: (*a*) C. L. Ren, F. Zhou, B. Qin, R. J. Ye, S. Shen, H. B. Su and H. Q. Zeng, *Angew. Chem., Int. Ed.*, 2011, **50**, 10612; (*b*) C. L. Ren, S. Y. Xu, J. Xu, H. Y. Chen and H. Q. Zeng, *Org. Lett.*, 2011, **13**, 3840. For pyridone-based foldamers, see: (*c*) C. L. Ren, V. Maurizot, H. Q. Zhao, J. Shen, F. Zhou, W. Q. Ong, Z. Y. Du, K. Zhang, H. B. Su and H. Q. Zeng, *J. Am. Chem. Soc.*, 2011, **133**, 13930; (*d*) Z. Y. Du, C. L. Ren, R. J. Ye, J. Shen, Y. J. Lu, J. Wang and H. Q. Zeng, *Chem. Commun.*, 2011, **47**, 12488. For pyridine-based foldamers, see: (*e*) W. Q. Ong, H. Q. Zhao, Z. Y. Du, J. Z. Y. Yeh, C. L. Ren, L. Z. W. Tan, K. Zhang and H. Q. Zeng, *Chem. Commun.*, 2011, **47**, 6416; (*f*) W. Q. Ong, H. Q. Zhao, X. Fang, S. Woen, F. Zhou, W. L. Yap, H. B. Su, S. F. Y. Li and H. Q. Zeng, *Org. Lett.*, 2011, **13**, 3194; (*g*) H. Q. Zhao, W. Q. Ong, X. Fang, F. Zhou, M. N. Hii, S. F. Y. Li, H. B. Su and H. Q. Zeng, *Org. Biomol. Chem.*, 2012, **10**, 1172.

7 For some representative examples on macrocycles of diversestructures by others, see: (*a*) F. J. Carver, C. A. Hunter and R. J. Shannon, *Chem. Commun.*, 1994, 1277; (*b*) H. Jiang, J. M. Leger, P. Guionneau and I. Huc, *Org. Lett.*, 2004, **6**, 2985; (*c*) J. K. H. Hui and M. J. MacLachlan, *Chem. Commun.*, 2006, 2480; (*d*) J. B. Lin, X. N. Xu, X. K. Hang and Z. T. Li, *J. Org. Chem.*, 2008, **73**, 9403; (*e*) A. Petitjean, L. A. Cuccia, M. Schmutz and J. M. Lehn, *J. Org. Chem.*, 2008, **73**, 2481; (*f*) Y. Y. Zhu, C. Li, G. Y. Li, X. K. Jiang and Z. T. Li, *J. Org. Chem.*, 2008, **73**, 1745; (*g*) H. C. Ahn, S. M. Yun and K. Choi, *Chem. Lett.*, 2008, **37**, 10; (*h*) W. Feng, K. Yamato, L. Q. Yang, J. S. Ferguson, L. J. Zhong, S. L. Zou, L. H. Yuan, X. C. Zeng and B. Gong, *J. Am. Chem. Soc.*, 2009, **131**, 2629; (*i*) J. S. Ferguson, K. Yamato, R. Liu, L. He, X. C. Zeng and B. Gong, *Angew. Chem., Int. Ed.*, 2009, **48**, 3150; (*j*) F. Li, Q. Gan, L. Xue, Z.-M. Wang and H. Jiang, *Tetrahedron Lett.*, 2009, **50**, 2367; (*k*) C. Han, F. Ma, Z. Zhang, B. Xia, Y. Yu and F. Huang, *Org. Lett.*, 2010, **12**, 4360; (*l*) Z. Zhang, Y. Luo, B. Xia, C. Han, Y. Yu, X. Chena and F. Huang, *Chem. Commun.*, 2011, **47**, 2417.

8 The bulk of the computational analysis in this section has been described in the ESI of ref. 5*h* and applied to the gas phase, $CHCl_3$ and THF. We now fully extended it to other solvent systems (acetone, acetonitrile and DMSO) with additional discussions as well as further incorporated Table 4 to illustrate the reliability of the obtained E_O and E_M values.

9 *Mathematica, 7.0 ed*, Wolfram Research, Inc., Champaign, IL, 2008.